Current Research in Food Science 8 (2024) 100760

Contents lists available at ScienceDirect

Current Research in Food Science

journal homepage: www.sciencedirect.com/journal/current-research-in-food-science

In vitro digestion and fermentation behaviors of polysaccharides from *Choerospondias axillaris* fruit and its effect on human gut microbiota

Jinjiao Dong [a,1], Wenjun Wang [a,1], Guodong Zheng [a], Nansheng Wu [b], Jingjing Xie [a], Shiyi Xiong [a], Panting Tian [c], Jingen Li [a,*]

[a] College of Food Science and Engineering, Jiangxi Agricultural University, Nanchang, 330045, China
[b] Choerospondias Axillaris Research Institute, Jiangxi Agricultural University, Nanchang, 330045, China
[c] Jiangxi Qiyunshan Food Co., Ltd, China

ARTICLE INFO

Keywords:
Polysaccharides
Choerospondias axillaris fruit
In vitro digestion
In vitro fermentation
Gut microbiota

ABSTRACT

Choerospondias axillaris fruit has attracted more and more attention due to its various pharmacological activities, which are rich in polysaccharides. This study investigated the *in vitro* saliva-gastrointestinal digestion and fecal fermentation behaviors of polysaccharides from *Choerospondias axillaris* fruit (CAP), as well as its impact on human gut microbiota. The results showed that CAP could be partially degraded during the gastrointestinal digestion. The FT-IR spectra of the digested CAP didn't change significantly, however, the morphological feature of SEM changed to disordered flocculent and rod-like structures. 16S rRNA sequencing analysis found that after *in vitro* fermentation, CAP could increase the relative abundances of beneficial bacteria including *Megasphaera*, *Megamonas* and *Bifidobacterium* to produce short-chain fatty acids (SCFAs), while it can also reduce the abundances of harmful bacteria of *Collinsella*, *Gemmiger*, *Klebsiella* and *Citrobacter*, suggesting that CAP could modulate the composition and abundance of gut microbiota. These results implied that CAP can be developed as a potential prebiotic in the future.

1. Introduction

The human digestive system is home to a complex and dynamic community of microorganisms referred to as the gut microbes or gut flora, which have a significant impact on host health and disease (Paliy et al., 2009). More recent studies have linked dysregulation of the gut microbiota to a number of diseases, such as inflammatory bowel disease, diabetes, cirrhosis, depression, and so on. Numerous factors have impacts on the composition of gut flora, such as nutrition, health state, geography, polluted environments, genetics et al. (Shang, et al., 2018) Among them, nutrition is commonly regarded as an extremely essential element (Oriach et al., 2016). Studies proved that chronic high-fat and high-sugar diets led to the extinction of several taxa of the gut microbiota, therefore affecting the immune system, nervous system, metabolic diseases et al. (Sherwin et al., 2018). As symbiotic bacteria, gut microbiota can use indigestible fibers and polysaccharides as energy sources, as well as produce some metabolites that are beneficial to human health, for instance, short-chain fatty acids (Shang, et al., 2018).

Polysaccharides are widely distributed in animals, plants and microorganism. Due to their good efficacy and low toxicity, natural polysaccharides are usually used in the health products industry, and it has been reported to possess good antioxidant, anti-tumor, hypoglycemic and immune activities (Xie et al., 2023). However, increasing evidence suggested that plant polysaccharides are resistant to upper digestive tract hydrolysis, but can be decomposed and utilized by microbes in the distal gut, thereby maintaining *in vivo* ecological balance (Rao & Quartarone, 2019). Due to the complex chemical structure, different polysaccharides have different digestion and glycolysis characteristics, which are crucial for their bioactivities after oral ingestion. *In vitro* simulated digestion method was often used to study the stability, bioactivity, and bioavailability of polysaccharides due to its convenience and good repeatability. Meanwhile, *in vitro* fecal fermentation was used to assess the contribution of polysaccharides to the growth of gut microbiota and their functions (Pérez-Burillo, et al., 2021).

Choerospondias axillaris (*C. axillaris*), also known as the Nepali hog plum, is a member of the *Anacardiaceae* family, which is extensively

* Corresponding author.
E-mail address: enen928@163.com (J. Li).
[1] These authors have contributed equally to this work.

https://doi.org/10.1016/j.crfs.2024.100760
Received 22 February 2024; Received in revised form 22 April 2024; Accepted 3 May 2024
Available online 6 May 2024

spread in Nepal, Japan, India, and China (Mann et al., 2022). *C. axillaris* fruits are usually used both as food and medicine in folk for a long time. For instance, the dry mature fruits have been used to treat cardiovascular diseases since ancient times (Wang et al., 2008), while the fresh fruits were more often used to produce juice and cake rather than being eaten raw due to its sour taste (Li, et al., 2022). In addition, the fresh fruits of *C. axillaris* are often used for appetizing and invigorating the spleen, promoting digestion, relieving food stagnation, and relaxing bowel by the local residents. However, the underlying mechanism is not clear yet. It has been confirmed that *C. axillaris* fruits contain numerous bioactive compounds, such as polyphenolics, proanthocyanidins, polysaccharides, and flavonoids, which exhibit various biological activities. The water extract of *C. axillaris* fruits has significant DPPH and O_2^- free radical scavenging ability and reducing ability (Wang et al., 2008). Total flavonoids extracted from *C. axillaris* fruits can alleviate cardiac dysfunction and myocardial interstitial fibrosis through NF-κB signaling pathway, which has antiarrhythmic effect (Qiu, et al., 2016; Sun et al., 2014). Proanthocyanidins from *C. axillaris* are a good source of angiogenesis inhibitors (Li, et al., 2016).

According to our previous studies, water-soluble polysaccharides (CAP) are the major bioactive constituents in the *C. axillaris* fruits with an approximate yield of 21.79%, and it exhibited remarkable *in vitro* antioxidant, hypoglycemic and hypolipidemic effects (Li et al., 2024; Li et al., 2017). *In vitro* digestion properties of CAP were examined by the simulated digestion models. Anaerobic fecal fermentation model was applied to determine whether there were interactions between CAP and the human gut microbiota. 16S rRNA gene sequencing and gas chromatography (GC) were applied to determine the effects of CAP on the human gut microbiota and the production of short-chain fatty acids (SCFAs). The results help to understand the *in vitro* digestion and fecal fermentation characteristics of CAP and provide a scientific foundation for the development of this new plant polysaccharides as prebiotics.

2. Materials and methods

2.1. Materials and reagents

C. axillaris fruit was purchased from Ganzhou, Jiangxi Province, China. α-amylase, pepsin, trypsin and monosaccharide standards (*L*-fucose, *L*-Fuc; *L*-rhamnose, *L*-Rha; *L*-arabinose, *L*-Ara; *D*-glucosamine, *D*-GlcN; *D*-glactose, *D*-Gal; *D*-glucose, *D*-Glc; *L*-xylose, *L*-Xyl; *D*-mannose, *D*-Man; *L*-fructose, *L*-Fru; *D*-galacturonic acid, *D*-GalA; *D*-guluronic acid, *D*-GulA) were purchased from Shanghai Yuanye Bio-Technology Co., Ltd (Shanghai, China). Pancreatin was purchased from Sigma Chemical Co. (St. Louis, MO, USA). Inulin, resazurin and fatty acid standard (acetic acid, propionic acid, *i*-butyric acid, *n*-butyric acid, *i*-valeric acid, *n*-valeric acid, *n*-hexanoic acid) were bought from Shanghai Aladdin Biochemical Technology Co., Ltd (Shanghai, China). Cysteine, heme chloride, pig bile salt and Tween-80 were from Beijing Solarbio Science & Technology Co.,Ltd. (Beijing, China). Dextran standards (M_w 1152, 5000, 11600, 23800, 48600, 80900, 148000, 273000 Da) were bought from Sigma Chemical Co. Ltd. (St. Louis, MO, USA).

2.2. Isolation of CAP

CAP was isolated according to our previous report (Li et al., 2018). Briefly, the dry fruit pulp powders were extracted at 100 °C for 5 h in a material-to-liquid ratio of 1:40 (g/mL). The extraction solution was filtered and concentrated, and then precipitated with four volumes of anhydrous ethanol. The precipitate of polysaccharide was collected by centrifugation at 4000 rpm for 20 min, and then washed with anhydrous ethanol for three times. After drying under vacuum, CAP was obtained, which contained 46.5 ± 0.24% of total sugar, 63.71 ± 0.17% of uronic acid and 0.72 ± 0.02% of protein.

2.3. In vitro digestion of CAP

In vitro digestion of CAP was performed according to the published methods (Li, et al., 2020; Ma et al., 2022), with minor modifications. Firstly, the saliva electrolyte solution (SES), gastric electrolyte solution (GES) and small intestine electrolyte solution (SIES) were prepared. The SES was prepared by weighing 0.15 g NaCl, 0.03 g $CaCl_2$, 0.3 g KCl into 200 mL distilled water, and the pH was adjusted to 7 with 0.1 mol/L HCl or 0.1 mol/L $NaHCO_3$. The GES was prepared with 0.64 g NaCl, 0.22 g KCl, 0.03 g $CaCl_2{\cdot}2H_2O$ and 0.12 g $NaHCO_3$ into 200 mL of distilled water, and the pH was adjusted to 3.0 with 1 mol/L HCl. The SIES (200 mL) contained 1.08 g NaCl, 0.13 g KCl and 0.066 g $CaCl_2{\cdot}2H_2O$, the pH of which was neutralized to 7 with 1 mol/L $NaHCO_3$. Secondly, the artificial saliva juice (pH 7) was made by adding 0.86 g α-amylase into 200 mL of SES. The artificial gastric juice (pH 3) was made by adding 0.0656 g gastric pepsin and 1.5 mL CH_3COONa solution (1 mol/L) into 150 mL of GES. The artificial intestinal juice (pH 7) was prepared by adding 20 mL mixture of pancreatin (7%, w/v), 40 mL pig bile salt solution (4%, w/v) and 26 mg trypsin into 20 mL SIES. Finally, *in vitro* digestion was conducted by incubating CAP with the artificial digestion juice. For the salivary digestion (S), 4 mL of CAP solution (25 mg/mL) was incubated with 4 mL of artificial saliva juice at 37 °C for 5, 15 and 30 min. For the saliva-gastric digestion (SG), 6 mL of S (5 min) was incubated with 6 mL of artificial gastric juice at 37 °C for 1, 3 and 6 h. After the SG samples were collected, the pH was adjusted to 7 with 0.1 mol/L $NaHCO_3$ immediately. For the saliva-gastrointestinal digestion (SGI), 12 mL of SG (2 h, pH 7) was mixed with 3.6 mL of artificial intestinal juice in a ratio of 10:3 (v/v), and they were incubated at 37 °C for 1, 3 and 6 h. All the digestive enzymes were inactivated by boiling for 10 min to end the simulated digestion.

All the digestion samples were centrifuged at 4000 rpm for 10 min. The supernatants were collected for the reducing sugar and molecular weight analysis, and then the rest supernatants were precipitated with four volumes of anhydrous ethanol, and the precipitates were redissolved, dialyzed (8–14 kDa) and lyophilized to obtain different digestion products, which were designated as CAP-S, CAP-SG and CAP-SGI, respectively.

2.4. Physico-chemical properties of digested CAP

2.4.1. Reducing sugar

The reducing sugar concentration was determined using the 3,5-dinitrosalicylic acid (DNS) approach (Miller, 1959). Briefly, 200 μL digestion supernatant was mixed with 400 μL DNS reagent, and heated at 95 °C for 2 min, with glucose as standard. After cooling to room temperature, the solution was diluted for four times and a microplate reader was used to determine the absorbance at 540 nm.

2.4.2. Molecular weight

The molecular weight of CAP, CAP-S, CAP-SG and CAP-SGI were measured by a Shimadzu LC-10A high-performance size exclusion chromatography (HPSEC) system (Tokyo, Japan) equipped with two size exclusion chromatography columns in series (SB-806 HQ, SB-804 HQ, 8 × 300 mm, Japan) and an Optilab T-rEX differential refractive index detector (dRID, Wyatt Technology Corporation, CA, United States). The mobile phase was 0.1 mol/L sodium nitrite solution containing 0.02% (w/w) sodium azide with a flow rate of 0.6 mL/min. The column temperature was 35 °C, the sample volume was 50 μL, and the running time was 80 min. The weight-average molecular weight (M_w) and number-average molecular weight (M_n) were calculated by the calibration curves of standard dextrans.

2.4.3. Monosaccharide composition

2 mg of dry CAP, CAP-S, CAP-SG and CAP-SGI were hydrolyzed by 3 mL trifluoroacetic acid solution (2 mol/L) at 110 °C for 4 h. After that, the solution was blow-dried by a nitrogen stream at 50 °C, and then 3 mL

methanol was added and blow-dried again, which was repeated for at least four times. The samples were then dissolved in 2 mL of distilled water and passed through a 0.22 μm membrane, and then examined by a Dionex ICS-5000+ high-performance anion exchange chromatography (HPAEC) system (Thermo Fisher Scientific Inc., US) equipped with a Dionex Carbopac™ PA20 column (3 mm × 150 mm, Dionex Corporation, US) and a pulsed amperometric detector (PAD) according to the method described in our earlier work (Li et al., 2017). The standard curves were plotted using eleven monosaccharide standards, and the molar ratios were computed based on the peak areas.

2.4.4. Fourier transform infrared spectroscopy (FT-IR)

Approximately 1 mg of CAP samples and 100 mg of dried KBr powder (spectrographically pure grade) were mixed uniformly and pressed into a 1 mm slice. A Nicolet iS5 spectrometer (Thermo Fisher Scientific, USA) was used for FT-IR analysis, and the frequency range was from 4000 to 400 cm^{-1}.

2.4.5. Scanning Electron Microscopy (SEM)

The freeze-dried samples were sprayed with gold under vacuum after being adhered to a support with adhesive tape. The observations were captured by a Scanning Electron Microscope (Hitachi SU8020, Japan) at magnifications of 500 × and 1000 × .

2.5. In vitro fermentation of CAP

2.5.1. In vitro fermentation using human fecal inoculum

The *in vitro* fermentation of CAP was carried out according to the reported method (Wu, et al., 2021). Firstly, a basic culture medium was prepared by dissolving 2 g peptone, 2 g yeast extract, 0.8 g *L*-cysteine-HCl·H_2O, 4.5 g NaCl, 4.5 g KCl, 1.5 g $NaHCO_3$, 0.5 g K_2HPO_4, 0.04 g KH_2PO_4, 0.69 g $MgSO_4$·H_2O, 0.08 g $CaCl_2$, 0.005 g $FeSO_4$·$7H_2O$, 0.4 g pig bile salt, 1 mL Tween 80, and 2 mL resazurin (0.01%, w/v) into 1000 mL distilled water. After fully mixing, the medium was sterilized for 15 min at 121 °C. After the pH was adjusted to 7 by 2 mol/L HCl, 0.02 g heme chloride was added. Secondly, fresh feces from four healthy volunteers (20–28 years old, two females and two men) who had not taken antibiotics or prebiotic therapy for at least three months were collected and combined uniformly in equal amounts. The feces were diluted with sterile phosphate buffer to make a 10% (w/v) fecal slurry, and then the solid residues were removed by filtering through a four layers of gauze. Finally, 13 mL of basic culture medium and 2 mL 10% fecal slurry were mixed uniformly in a fermentation flask with nitrogen filling, and 0.1 g distilled water, CAP and inulin were added as BLK group, CAP group and INL group, respectively. In addition, the original 10% fecal slurry without any treatment was set as ORS group. The samples were further incubated in a shaker (120 rpm) at 37 °C for 0, 6, 12, 24, and 48 h. Each trial was carried out three times.

2.5.2. pH and OD_{600}

The pH values of fermentation liquid at 0, 6, 12, 24 and 48 h were determined with a pH meter. After the fermentation liquid was centrifuged for 10 min (4 °C, 14000 rpm), the supernatant was deserted, and the residues were resuspended by 0.4 mL of sterile saline. The absorbance value of OD_{600} was measured, which represented the bacterial density (Guo, et al., 2022).

2.5.3. Total sugars, uronic acids and reducing sugars

The concentrations of total sugars and uronic acids in the fermentation liquid were determined by phenol-sulfuric acid and sulfuric acid-carbazole methods (Ma et al., 2021), with *D*-Glc and *D*-GalA as standards, respectively. The reducing sugars concentration was determined according to the DNS method described in 2.4.1.

2.5.4. Analysis of fecal microbiota

After 48 h fermentation, total DNA of fecal microbiota was extracted using the TIANamp Stool DNA Kit (Tiangen Biochemical Technology Co., Ltd., Beijing, China) according to the manufacturer's instructions. The V3–V4 regions of 16S rRNA were used for amplification and then sequenced by Shanghai Personal Biotechnology Co., Ltd (Shanghai, China). All the data was analyzed using the online platform of genes Cloud Platform (https://www.genescloud.cn).

2.5.5. SCFAs extraction and analysis

According to the method of Guan et al. (2022), 0.4 mL fermentation solution was mixed uniformly with an equal volume of ethyl acetate for 30 s by a vortex oscillator. The mixture was centrifuged for 10 min at 12000 rpm, and then the supernatant was filtered through a 0.22 μm membrane. The composition of short-chain fatty acids (SCFAs) was determined by an Agilent 7890 gas chromatography (GC) (Agilent Technologies, 7890B, USA) coupled with an Agilent ZORBAX Eclipse Plus-C18 column (30 m × 0.25 mm × 0.25 μm, CA, USA) and a flame ionization detector (FID). The flow rate of carrier gas (nitrogen, >99.999%) was 2 mL/min. The initial column temperature was kept at 100 °C for 1 min and then raised to 150 °C at a rate of 5 °C/min. The temperature of injector and detector were both kept at 250 °C. Air, nitrogen, and hydrogen were employed as make-up gases, with flow rates of 400, 25 and 40 mL/min, respectively.

2.6. Statistical analysis

All data were expressed as mean ± standard deviation (SD). Significant differences were performed using post hoc Duncan's test and one-way analysis of variance (ANOVA) at $P < 0.05$ level (SPSS 26.0 software, SPSS Inc., Chicago, IL, USA).

3. Results and discussions

3.1. In vitro digestion of CAP

3.1.1. Reducing sugars, molecular weight and monosaccharides composition changes

Generally, the breakdown of glycosidic bonds in polysaccharides caused the increase of reducing sugar. As shown in Table 1, the reducing sugar of CAP increased slightly from 0.939 ± 0.013 mg/mL to 1.032 ± 0.048 mg/mL during the salivary digestion, and it significantly reached 1.286 ± 0.164 mg/mL after 6 h of gastric digestion ($P < 0.05$). It was later significantly increased from 1.182 ± 0.022 mg/mL to 1.764 ± 0.098 mg/mL after 6 h of intestinal digestion ($P < 0.05$). The results indicated that the degradation of CAP mainly happened in the gastrointestinal tract, which could be attributed to the low pH of gastric juices and the activity of other digestive enzymes (Hu et al., 2013).

The dynamic variation in molecular weights during *in vitro* digestion process was studied. Fig. 1A depicted that CAP exhibited a single

Table 1
The dynamic changes of molecular weight and reducing sugar of CAP during *in vitro* digestion.

Samples	M_w(kDa)	M_n(kDa)	M_w/M_n	Reducing sugar (mg/mL)
CAP	66.30	42.88	1.566	
CAP-S-5min	61.94	41.32	1.499	0.939 ± 0.013^{d}
CAP-S-15min	61.63	39.10	1.579	1.008 ± 0.010^{cd}
CAP-S-30min	60.34	38.96	1.855	1.032 ± 0.048^{cd}
CAP-SG-1h	53.56	34.34	1.566	1.005 ± 0.036^{cd}
CAP-SG-3h	57.65	36.82	1.560	1.194 ± 0.236^{bc}
CAP-SG-6h	49.71	25.98	1.913	1.286 ± 0.164^{b}
CAP-SGI-1h	49.51	26.69	1.549	1.182 ± 0.022^{bc}
CAP-SGI-3h	22.08	13.28	1.662	1.304 ± 0.098^{b}
CAP-SGI-6h	24.58	12.90	1.905	1.764 ± 0.098^{a}

Values represent mean ± standard deviation (SD, n = 3) and values within the same column with different alphabets (a-d) indicate significantly different ($P < 0.05$).
M_w, weight average molecular weight; M_n, number average molecular weight.

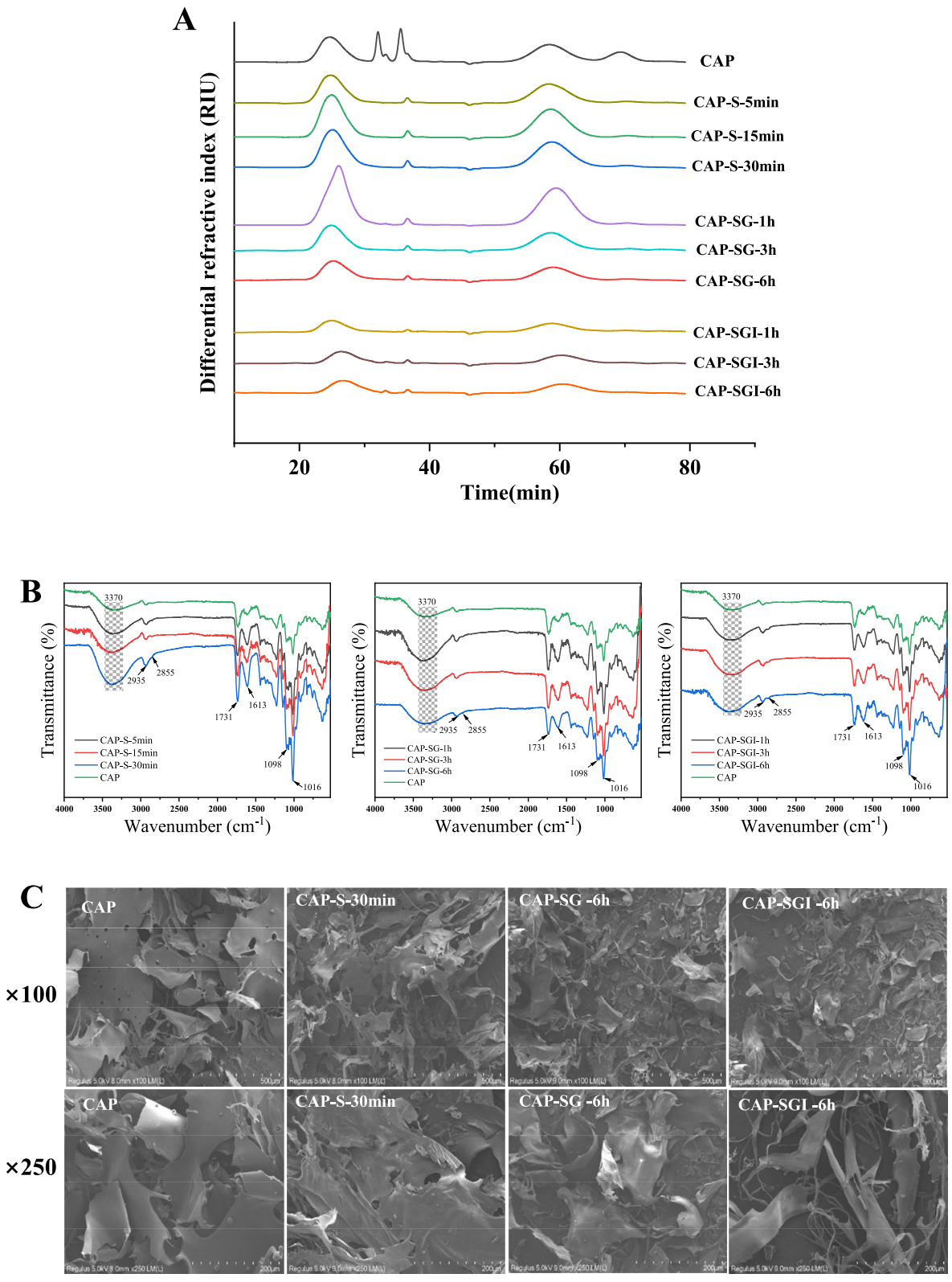

Fig. 1. Dynamic changes of M_w (A), FT-IR spectra (B) and SEM images (C) of CAP during *in vitro* digestion. CAP, polysaccharides from *Choerospondias axillaris* fruit; CAP-S, CAP-SG, and CAP-SGI indicated CAP was digested by salivary digestion, saliva-gastric digestion, and saliva-gastrointestinal digestion, respectively.

symmetric peak (Fraction I, 20–30 min) and two small peaks (Fraction II and III, 30–40 min). The retention time of Fraction I increased and Fraction II & III almost disappeared, also indicating that the CAP was degraded during the saliva-gastrointestinal digestion. Accordingly, Table 1 displayed the weight-average molecular weight (M_w), number-average molar mass (M_n) and polydispersities (M_w/M_n). From Table 1, the M_w of CAP decreased slightly from 66.30 to 60.34 kDa after 30 min of salivary digestion. However, the M_w dropped dramatically from 53.56 to 24.58 kDa ($P < 0.05$) after gastrointestinal digestion. According to previous reports, the molecular loss of CAP may be caused by the acidic

environment of the stomach as well as large quantities of digestion enzymes and bile salts or other aggregates in the intestinal juice (Chen, et al., 2018). Moreover, the polydispersities (M_w/M_n) of CAP, CAP-S-30min, CAP-SG-6h, and CAP-SGI-6h were 1.566, 1.855, 1.913, and 1.905, respectively, which were agreed with the HPSEC result. A peak around 60 min was the solvent signal.

The dynamic changes of monosaccharides were shown in Table 2. It indicated that CAP was composed of *L*-Rha, *L*-Ara, *D*-Gal, *D*-Glc and *D*-GalA. *L*-Ara and *D*-Glc decreased significantly, suggesting that they were likely to be the end residues of the sugar chain, which were sensitive to the digestive fluid. On the contrary, *L*-Rha, *D*-Gal and *D*-GalA increased mildly, implying that they might be as the backbone of CAP that were more stable during the digestion process.

3.1.2. Changes in FT-IR and SEM spectra of CAP during in vitro digestion

The FT-IR spectra results (Fig. 1B) indicated that the structural characteristics of CAP didn't change significantly during the digestion. Briefly, the O–H stretching vibrations were responsible for the strong and broad absorption band at 3370 cm^{-1}. The characteristic peaks at 1098 and 1016 cm^{-1} were attributed to the glycosidic bond (C–O) and pyranoid ring, whereas the peaks at 2935 and 2855 cm^{-1} were corresponded to symmetric and asymmetric stretching vibrations of C–H (Fu, et al., 2023). In addition, two strong absorption peaks, representing the stretching vibrations of methyl esterified and non-esterified carboxyl groups, were found at 1731 and 1613 cm^{-1} (Fu, et al., 2023).These results indicated that although some glycosidic bonds were broken down, there was no significant difference in the major functional groups of CAP after digestion.

The SEM results (Fig. 1C) indicated that CAP had a lamellar structure with a smooth surface. However, the smooth surface morphology changed to rough after 30 min of salivary digestion, and it changed to a smaller size with curled edge by 6 h of gastric digestion. In addition, it changed to a disordered flocculent and rod-like structure after 6 h of intestinal digestion. The morphological changes may be caused by the interactions of polysaccharides with digestive enzymes, electrolytes, or the high-acidic environment in the gastrointestinal tract (Guo, et al., 2022).

3.2. In vitro fermentation of CAP

3.2.1. Changes of total sugars, uronic acids and reducing sugars

Generally, enzymes secreted from the gut microbiota could decompose the majority of indigestible polysaccharides to create reducing sugars, which could in turn used as carbon sources of the microorganism (Wu, et al., 2021). As shown in Table 3, the initial concentrations of total sugars, uronic acids and reducing sugars were 3.292 ± 0.254, 3.835 ± 0.196 and 1.674 ± 0.024 mg/mL, respectively. However, the total sugars and uronic acids decreased rapidly within 24 h fermentation. Meanwhile, the reducing sugars significantly increased from 1.674 ± 0.024 (0 h) to 1.858 ± 0.052 mg/mL (6 h), and then declined rapidly to 0.209 ± 0.003 mg/mL (48 h) ($P < 0.05$). These results indicated that CAP was decomposed by the fecal flora to create reducing sugars within 24 h, however, when the reducing sugars were further utilized by the microorganism, the concentration decreased accordingly at 48 h (Han, et al., 2022).

Table 2
Monosaccharides composition changes of CAP during *in vitro* digestion.

Sample	Molar ratio (%)				
	L-Rha	*L*-Ara	*D*-Gal	*D*-Glc	*D*-GalA
CAP-S-5min	2.20	3.21	5.74	3.41	85.44
CAP-S-15min	2.21	3.16	5.98	3.30	85.35
CAP-S-30min	2.16	3.27	6.37	3.34	84.86
CAP-SG-1h	1.98	2.92	5.66	3.44	86.00
CAP-SG-3h	1.93	2.68	5.35	2.46	87.58
CAP-SG-6h	2.15	3.09	5.62	3.01	86.13
CAP-SGI-1h	2.24	3.02	5.67	1.59	87.49
CAP-SGI-3h	2.30	2.77	4.92	2.81	87.20
CAP-SGI-6h	2.24	2.83	6.13	1.88	86.91

Table 3
Changes of total sugars, uronic acids and reducing sugars of CAP during *in vitro* fermentation.

Fermentation time (h)	Total sugars (mg/mL)	Uronic acids (mg/mL)	Reducing sugars (mg/mL)
0	3.292 ± 0.254[a]	3.835 ± 0.196[a]	1.674 ± 0.024[b]
6	1.871 ± 0.128[b]	2.826 ± 0.031[b]	1.858 ± 0.052[a]
12	0.835 ± 0.029[c]	1.151 ± 0.081[c]	0.948 ± 0.029[c]
24	0.428 ± 0.002[d]	0.332 ± 0.003[d]	0.163 ± 0.047[d]
48	0.461 ± 0.320[d]	0.356 ± 0.032[d]	0.209 ± 0.003[d]

Values represent mean ± SD (n = 3) and values within the same column with different alphabets (a-d) indicate significantly different ($P < 0.05$).

3.2.2. Changes of pH and OD_{600}

The pH value is a basic indicator to track the fermentation process of polysaccharides. As shown in Fig. 2A, there were no significant differences between groups at 0 h ($P < 0.05$), however, a significant declining trend was observed both in the INL and CAP groups ($P < 0.05$) as the increase of fermentation time. At 12 h, the pH declined significantly to 5.40 ± 0.021 (INL group) and 5.47 ± 0.015 (CAP group), respectively, while the pH of BLK group decreased slightly from 7.26 ± 0.015 (0 h) to 6.92 ± 0.006 (48 h). A decrease in pH was associated with an increase in SCFAs, and a low pH was conducive to microbial growth (Yin, et al., 2020).

In Fig. 2B, OD_{600} values of the INL and CAP groups increased markedly ($P < 0.05$) within 24 h fermentation. However, as the fermentation time increased, the upward trend slowed down from 24 to 48 h due to the consumption of the nutrient in the medium. The result indicated that the fecal microorganism grew rapidly with the inulin and CAP treatment.

3.2.3. Changes of gut microbiota after in vitro fermentation of CAP

3.2.3.1. Alpha and beta diversity analysis. As shown in Table 4, in order to assess community richness and diversity, Chao1, Observed_species, Shannon and Simpson indexes were determined. The CAP and INL groups have lesser community richness and variety when compared to the BLK group. Similar effects could be observed in the polysaccharides of *Paecilomyces cicadae* TJJ1213 and Chinese wolfberry, which could be explained by the dominating microbiota's competitive role (Tian, et al., 2023; Zhou et al., 2018).

Hierarchical clustering tree and principal co-ordinates analysis (PCoA) were examined to demonstrate the beta diversity of different groups. The cluster tree (Fig. 3A) showed that the four test groups aggregated into two branches, INL and CAP groups were grouped into one branch while BLK and ORS groups were grouped into another group. The PCoA result (Fig. 3B) indicated that the gut microbiota of CAP group was similar to the INL group, but distinct from the BLK and ORS groups. These findings indicated that there were significant disparities across groups.

3.2.3.2. Species differences between groups. A Venn plot was then used to show the common and unique OUT numbers of each group. As shown in Fig. 3C, there were 122 common OUTs overlapped and the ORS, BLK, INL and CAP groups had 696 (89.2%), 654 (60%), 353 (44.7%) and 298 (38.2%) unique OTUs, respectively.

Linear discriminant analysis (LDA) effect size (LEfSe) was carried out to explore the differential microbiota. The higher LDA scores, the greater contribution of the species to the abundance difference. As shown in Fig. 3D and E, the LEfSe analysis revealed that 35 biomarker taxa in total were determined with LDA score>4, and there were 15, 6, 5 and 9

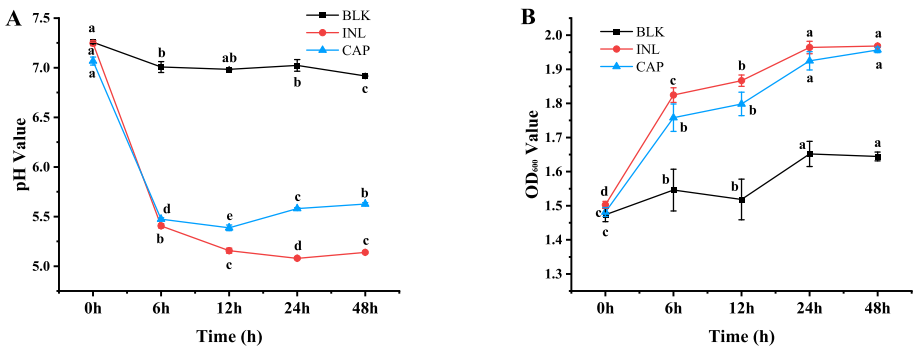

Fig. 2. Changes of pH (A) and OD_{600} (B) values during the *in vitro* fermentation.

Table 4
Alpha diversity of samples among different groups.

Group	Index			
	Chao1	Observed_species	Shannon	Simpson
ORS	561.452 ± 20.740	537.567 ± 35.154^{ab}	6.413 ± 0.037^{a}	0.964 ± 0.003^{a}
BLK	648.917 ± 96.507	611.367 ± 73.672^{a}	6.051 ± 0.108^{b}	0.943 ± 0.002^{ab}
INL	540.460 ± 46.440	479.633 ± 36.778^{b}	5.454 ± 0.045^{c}	0.923 ± 0.002^{b}
CAP	545.501 ± 84.011	491.73 ± 57.791^{b}	4.327 ± 0.157^{d}	0.759 ± 0.014^{c}

Values represent mean ± SD (n = 3) and values within the same column with different alphabets (a-d) indicate significantly different ($P < 0.05$).

dominant bacteria in ORS, BLK, CAP and INL groups, respectively. *Veillonellaceae*, *Megashaera*, *Clostridiales*, *Clostridia* and *Firmicutes* were the core bacteria of the CAP group. In INL group, *Bifidobacterium, Actinobacteria*, *Bifidobacteriaceae, Bifidobacteriales* and *Megamonas* were the characteristic bacteria. *Proteobacteria* was the dominant bacteria of the BLK group, which has been identified as a symptom of gut microbial dysbiosis and connected to a variety of diseases including diabetes, low-grade inflammation and colon cancer (Huang, et al., 2020). However, *Proteobacteria* was significantly reduced by CAP and INL treatment, while the abundance of *Firmicutes* and *Megashaera* were improved, which can decompose polysaccharides to produce SCFAs (Bai, et al., 2023).

3.2.3.3. Effects of CAP on microbial composition at the phylum and genus level. In order to investigate the impact of CAP on fecal microbiota, the microbial composition both at the phylum and genus levels was determined. As shown in Fig. 3F, *Firmicutes, Actinobacteria, Proteobacteria* and *Bacteroidetes* were the dominant bacteria in human feces, and the relative percentages of phyla changed with different treatments. Compared with the BLK and ROS groups, the abundance of *Firmicutes* in the INL and CAP groups significantly increased, while *Actinobacteria, Proteobacteria* and *Bacteroidetes* decreased, and these results were consistent with Han's study (Han, et al., 2022). *Bacteroides* have been reported to induce glucose intolerance in mice (Kovatcheva-Datchary, et al., 2015), which implied that CAP may help maintain the glucose homeostasis by down-regulating the abundance of *Bacteroides*. The results showed that CAP and INL could promote the proliferation of *Firmicutes*, which can produce SCFAs through the fermentation of indigestible carbohydrates in the colon leading to a declining pH (Chen, et al., 2018). On the other hand, a low pH is suitable for the growth of *Firmicutes* but may potentially inhibit the growth of *Bacteroides* (Chen, et al., 2023).

Moreover, the microbiota composition changes at the genus level were shown in Fig. 3G. The microbiota composition of BLK group was mainly composed of *Collinsella* and *Citrobacter*. Compared to the BLK group, the abundances of beneficial bacteria increase dramatically in the CAP and INL groups, for instance, *Megasphaera*, *Bifidobacterium* and *Megamonas*. Among them, *Megasphaera* was almost undetectable in the BLK and ORS groups. Studies revealed that *Megasphaera* can use glucose and lactic acid as substrates to produce hydrogen and carbon dioxide as byproducts, and it mainly produces propionic acid, butyric acid and valeric acid and vitamins, thus having potential for positive influence on host health (Wu, et al., 2021). *Bifidobacterium* is a well-known probiotic that can improve the intestinal environment and protect the intestinal tract from infection by pathogenic bacteria, which are essential for human gut health (Lv, et al., 2022). Many studies indicated that *Megamonas* is a unique genus that plays a pivotal role in the metabolism of carbohydrates into SCFAs and it also has a beneficial effect on patients undergoing metabolic syndromes, such as inflammation, cirrhosis and ischemia (Chen, et al., 2018). In addition, *Collinsella*, *Gemmiger*, *Klebsiella* and *Citrobacter* were reported as pathogens (Forbes, et al., 2018; Liang & Vallance, 2021; Olm et al., 2019; Ruiz-Limon, et al., 2022), and their abundance decreased in the CAP and INL groups. In sum, CAP played an essential role in regulating the gut microbiota by promoting good bacteria and inhibiting harmful bacteria. What's more, CAP exhibited a similar regulating effect on certain bacteria compared to INL, which was in line with the findings of an earlier study (Zhang, et al., 2022).

Heatmaps graphically represented the relative abundance of bacterial with defined color depths. As shown in Fig. 3H, compared with the ORS and BLK groups, CAP could increase *Firmicutes* and decrease *Actinobacteria*, *Proteobacteria, Fusobacteria* and *Synergistetes* at the phylum level. Studies have shown that *Proteobacteria* is always associated with pathogens (Zhang, et al., 2020). A low pH caused by fermentation can inhibit the growth of *Fusobacteria* (Feng, et al., 2022), which is closely linked to a number of diseases, such as cardiovascular disease and rheumatoid arthritis (Geng, et al., 2023). Meanwhile, as shown in Fig. 3I, CAP can significantly increase the abundance of *Pediococcus, Olsenella, Megasphaera, Sutterella,* and decrease the abundance of *Adlercreutzia, Dorea, Collinsella, Enterococcus, Gemmiger, Akkermansia* at the genus level. The above results demonstrated that CAP may regulate gut health by increasing the abundance of beneficial bacteria and reducing the abundance of harmful bacteria.

3.2.4. Changes in SCFAs

SCFAs are the primary metabolites of carbohydrates fermented by the gut microbiota, and they play a vital role in host health protection (Rui, et al., 2019). As indicated in Table 5, the total SCFAs of CAP group increased from 1.298 ± 0.020 (0 h) to 6.250 ± 0.183 mmol/L (48 h), which was significantly higher than the BLK group ($P < 0.05$). Acetic acid and propionic acid of CAP group increased significantly to 1.867 ± 0.248 and 2.559 ± 0.494 mmol/L at 6 h of fermentation, respectively. However, they decreased significantly ($P < 0.05$) from 6 h to 48 h, which may be attributed to the decrease of *Bacteroides* which primarily produce acetic acid and propionic acid (Gómez et al., 2016). Researches have indicated that acetic acid is an important energy source for peripheral

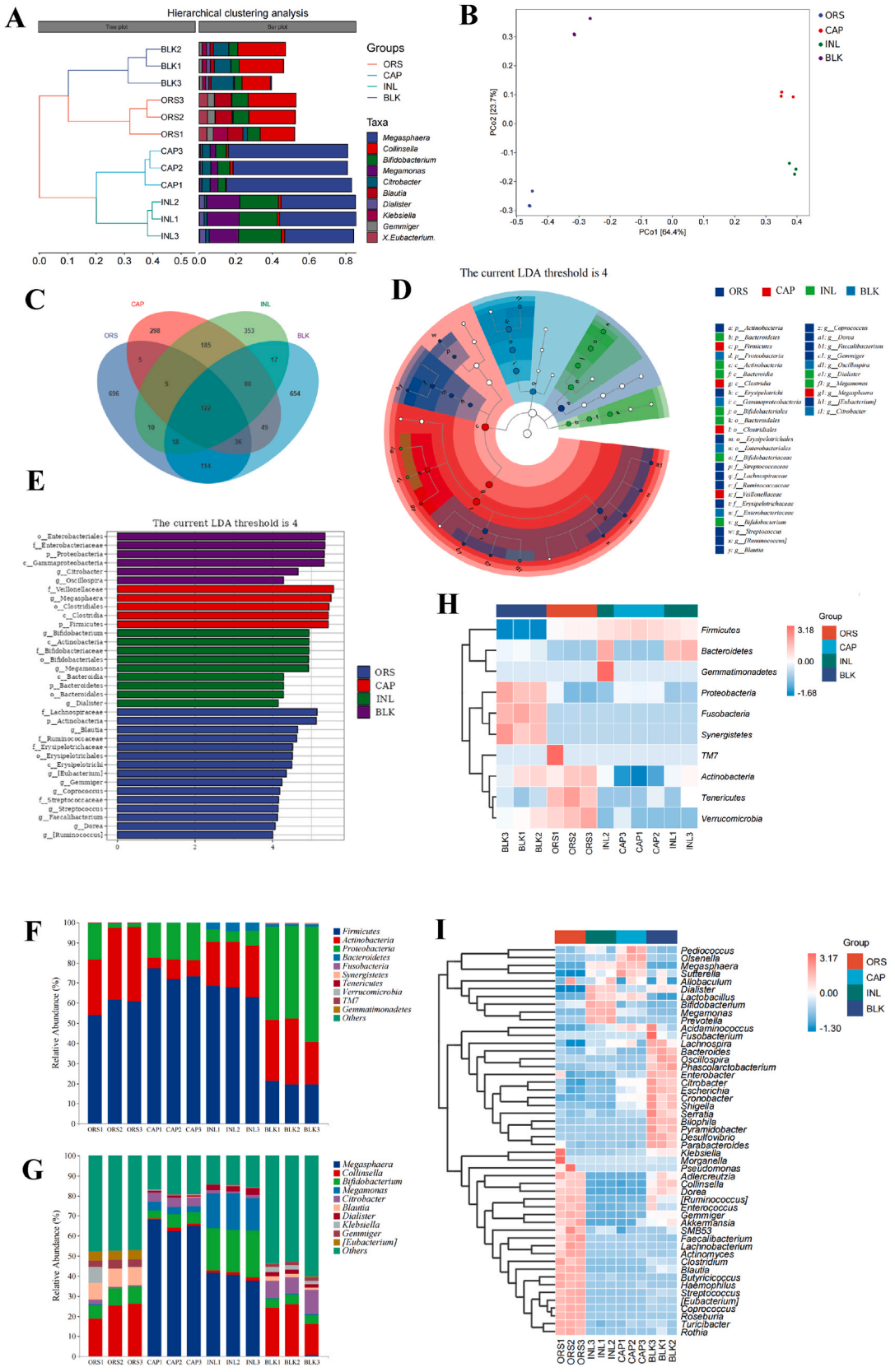

Fig. 3. Analysis of gut microbiota. Hierarchical clustering analysis (A); Principal co-ordinates (PCoA) analysis (B); Venn plot (C); LEfSe analysis (D); Histogram of LDA score (E); Microbiota composition of each group at the phylum level (F) and the genus level (G); Heatmap of species abundance at the phylum level (H) and the genus level (I).

Table 5
SCFAs changes during the *in vitro* fermentation.

Group	Time (h)	SCFAs(mmol/L)							
		acetic acid	propionic acid	i-butyric acid	n-butyric acid	i-valeric acid	n-valeric acid	n-hexanoic acid	Total SCFAs
CAP	0	0.441 ± 0.026^{d}	0.252 ± 0.006^{d}	0.119 ± 0.0003^{c}	0.212 ± 0.015^{e}	0.124 ± 0.010^{e}	0.083 ± 0.001^{d}	0.068 ± 0.004^{c}	1.298 ± 0.020^{c}
	6	1.867 ± 0.284^{a}	2.559 ± 0.494^{a}	0.123 ± 0.001^{c}	0.521 ± 0.670^{d}	0.521 ± 0.070^{d}	0.153 ± 0.015^{d}	0.065 ± 0.001^{c}	5.428 ± 0.868^{ab}
	12	1.522 ± 0.139^{b}	1.563 ± 0.213^{b}	0.138 ± 0.006^{b}	0.705 ± 0.116^{c}	0.705 ± 0.116^{c}	0.404 ± 0.096^{c}	0.071 ± 0.006^{c}	4.732 ± 0.655^{b}
	24	1.221 ± 0.051^{c}	0.982 ± 0.039^{c}	0.178 ± 0.003^{a}	1.539 ± 0.027^{b}	1.539 ± 0.027^{b}	1.284 ± 0.041^{b}	0.214 ± 0.002^{b}	5.885 ± 0.156^{a}
	48	1.143 ± 0.034^{c}	0.794 ± 0.037^{c}	0.180 ± 0.002^{a}	1.686 ± 0.059^{a}	1.686 ± 0.034^{a}	1.508 ± 0.050^{a}	0.428 ± 0.011^{a}	6.250 ± 0.183^{a}
INL	0	0.477 ± 0.04^{e}	0.247 ± 0.001^{d}	ND	0.206 ± 0.004^{e}	0.114 ± 0.001^{d}	0.091 ± 0.003^{d}	0.067 ± 0.001^{c}	1.202 ± 0.033^{d}
	6	2.089 ± 0.126^{d}	5.415 ± 0.280^{c}	0.122 ± 0.001^{c}	0.774 ± 0.063^{d}	0.146 ± 0.006^{d}	0.218 ± 0.019^{d}	0.072 ± 0.003^{c}	8.836 ± 0.496^{c}
	12	3.602 ± 0.160^{b}	9.435 ± 0.660^{b}	0.130 ± 0.003^{b}	1.201 ± 0.175^{c}	0.211 ± 0.013^{c}	0.707 ± 0.091^{c}	0.074 ± 0.002^{c}	15.489 ± 1.084^{b}
	24	4.602 ± 0.149^{a}	10.644 ± 0.217^{a}	0.214 ± 0.004^{a}	2.780 ± 0.043^{a}	0.701 ± 0.015^{a}	3.219 ± 0.050^{b}	0.111 ± 0.001^{b}	22.289 ± 0.458^{a}
	48	2.465 ± 0.100^{c}	5.138 ± 0.288^{c}	0.208 ± 0.005^{a}	2.224 ± 0.140^{b}	0.546 ± 0.038^{b}	3.558 ± 0.385^{a}	0.192 ± 0.012^{a}	14.331 ± 0.961^{b}
BLK	0	0.375 ± 0.041^{b}	0.280 ± 0.005^{b}	ND	0.202 ± 0.004^{c}	ND	0.101 ± 0.006^{c}	ND	0.959 ± 0.024^{c}
	6	0.420 ± 0.005^{ab}	0.271 ± 0.003^{b}	ND	0.204 ± 0.006^{c}	0.114 ± 0.001^{d}	0.092 ± 0.003^{d}	ND	1.100 ± 0.012^{b}
	12	0.484 ± 0.023^{a}	0.439 ± 0.010^{a}	ND	0.242 ± 0.005^{ab}	0.178 ± 0.003^{c}	0.113 ± 0.002^{b}	0.072 ± 0.001	1.527 ± 0.034^{a}
	24	0.465 ± 0.085^{a}	0.280 ± 0.010^{b}	0.122 ± 0.001	0.236 ± 0.008^{b}	0.213 ± 0.020^{b}	0.113 ± 0.002^{b}	0.075 ± 0.002	1.5047 ± 0.127^{a}
	48	0.432 ± 0.016^{ab}	0.281 ± 0.003^{b}	0.130 ± 0.001	0.248 ± 0.005^{a}	0.256 ± 0.006^{a}	0.128 ± 0.002^{a}	0.074 ± 0.003	1.549 ± 0.013^{a}

Values represent mean ± SD (n = 3) and values within the same column with different alphabets (a-e) indicate significantly different ($P < 0.05$). ND, not detected.

tissues and the brain, and it also regulates the fat insulin signaling and plays a key role in fat production and cholesterol synthesis in the host (Geng, et al., 2023). Propionic acid can inhibit cholesterol synthesis, enhance the sensitivity of insulin and exert anti-immunosuppression function (Laparra & Sanz, 2010). It was noted that after 48 h fermentation, *n*-butyric acid, *i*-valeric acid and *n*-valeric acid contents of CAP group reached 1.686 ± 0.059, 1.686 ± 0.034 and 1.508 ± 0.050 mmol/L, respectively, which were significantly higher than the BLK group ($P < 0.05$). The increasing percentage of *Firmicutes* might be responsible for the rise of butyric acid (Chen, et al., 2023), which in turn can boost intestinal immunity, provide epithelial cells energy, and preserve the integrity of the intestinal barrier (Zhang, et al., 2023). Furthermore, except *i*-valeric acid and *n*-hexanoic acid, the other SCFAs of CAP group were all higher than the BLK group but lower than the INL group. The results showed that CAP had similar effects to INL, and the increased concentration of SCFAs was related to the decreased pH of the fermentation solution. It is speculated that CAP may act as a new prebiotic by increasing the relative abundance of microorganisms that can generate SCFAs.

3.2.5. Correlation between SCFAs and microbiota

The relationship between the relative abundance of major intestinal flora at the genus level and SCFAs was examined using Spearman correlation analysis, to help identify the intestinal flora that may be involved in the production of SCFAs. As illustrated in Fig. 4, *Megasphaera* had a positive correlation with *i*-butyric acid ($P < 0.05$), *n*-butyric acid ($P < 0.05$), *i*-valeric acid and *n*-hexanoic acid. *Megamonas* and *Lactobacillus* were positively correlated with acetic acid, propionic acid ($P < 0.05$), *i*-butyric acid, *n*-butyric acid, *i*-valeric acid ($P < 0.05$) and *n*-valeric acid ($P < 0.05$). *Prevotella* and *Bifidobacterium* had a positive correlation with acetic acid, propionic acid, *i*-butyric acid ($P < 0.05$), *n*-butyric acid ($P < 0.05$) and *n*-valeric acid. *Sutterella*, *Pediococcus* and *Olsenella* were positively correlated with *n*-hexanoic acid. *Dialister* and *Butyricicoccus* were positively correlated with propionic acid ($P < 0.05$). *Faecalibacterium* was positively correlated with *i*-butyric acid ($P < 0.05$), *n*-butyric acid, *i*-valeric acid and *n*-valeric acid ($P < 0.05$). A total of 32 bacteria (*Collinsella, Citrobaccter*, *Cronobacter*, *Escherichia*, *Dorea*, *Gemmiger*, *Blautia* and *Phascolarctobacterium,* etc.) were negatively correlated with SCFAs. In sum, it implied that CAP may improve the intestinal environment and enhance human immunity by promoting the growth of *Megasphaera*, *Megamonas* and *Bifidobacterium* to produce SCFAs.

3.2.6. Metabolic pathway prediction

In order to better understand the role of bacterial communities in these samples, KEGG pathway analysis was used to predict gene functions related to genomic information. Fig. 5A showed that, compared with the ORS group, pathways of Lipopolysaccharide biosynthesis, Styrene degradation and Geraniol degradation were significantly up-regulated ($P < 0.05$) in CAP group. However, Endocytosis, Sphingolipid metabolism and Amoebiasis pathways were significantly down-regulated ($P < 0.05$). Compared with the BLK group (Fig. 5B), N-Glycan biosynthesis, Styrene degradation and *D*-Arginine and *D*-ornithine metabolism pathways were significantly up-regulated ($P < 0.05$), while Chloroalkane and chloroalkene degradation, Sphingolipid metabolism, and Tropane, piperidine and pyridine alkaloid biosynthesis were significantly down-regulated ($P < 0.05$). Compared with the INL group (Fig. 5C), pathways of Carotenoid biosynthesis, Bacterial invasion of epithelial cells and Biosynthesis of siderophore group nonribosomal peptides were significantly up-regulated ($P < 0.05$), while then Chloroalkane and chloroalkene degradation, Apoptosis and Protein digestion and absorption pathways were significantly down-regulated ($P < 0.05$). In conclusion, it was hypothesized that CAP may enhance the gut microbiota metabolism, hence increasing the body's defense mechanisms.

4. Conclusion

In this research, the decreased of molecular weight and increased reducing sugar revealed that CAP could be partially decomposed during the gastrointestinal digestion. In addition, the decreased pH and

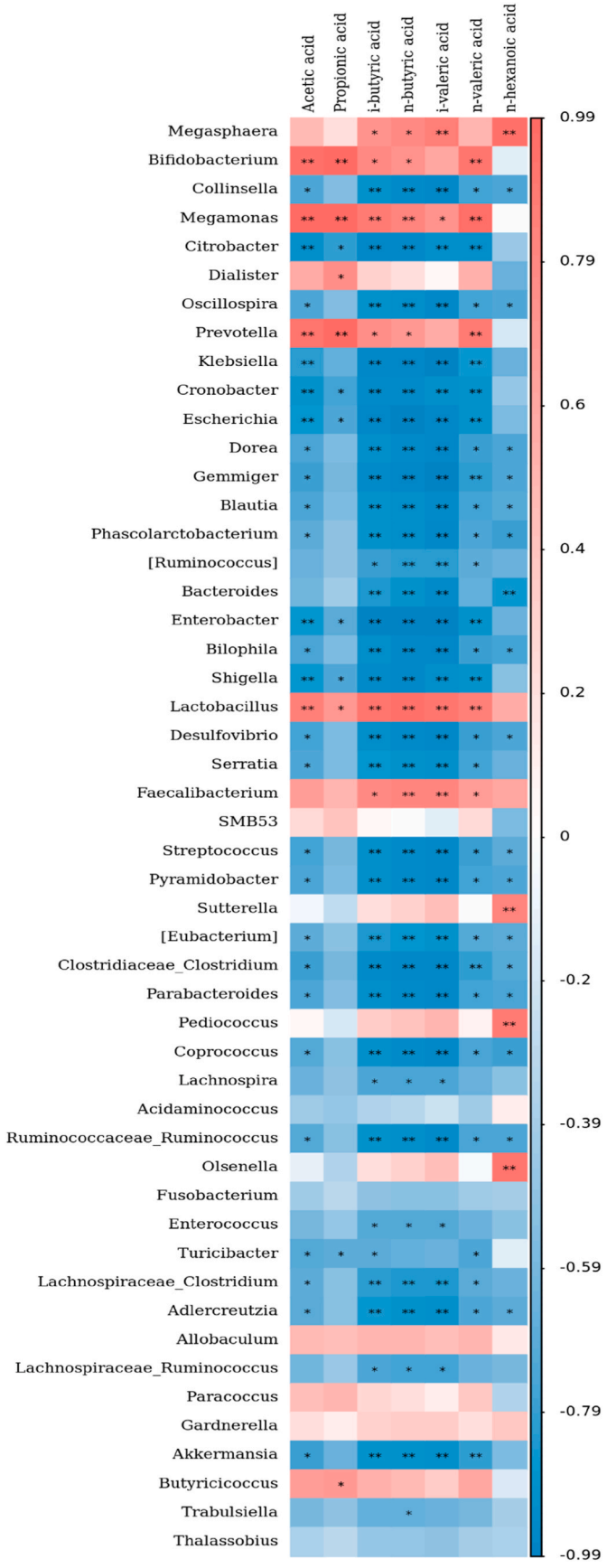

Fig. 4. Correlation analysis between SCFAs and the top 50 bacteria at genus level. *$P < 0.05$; **$P < 0.01$.

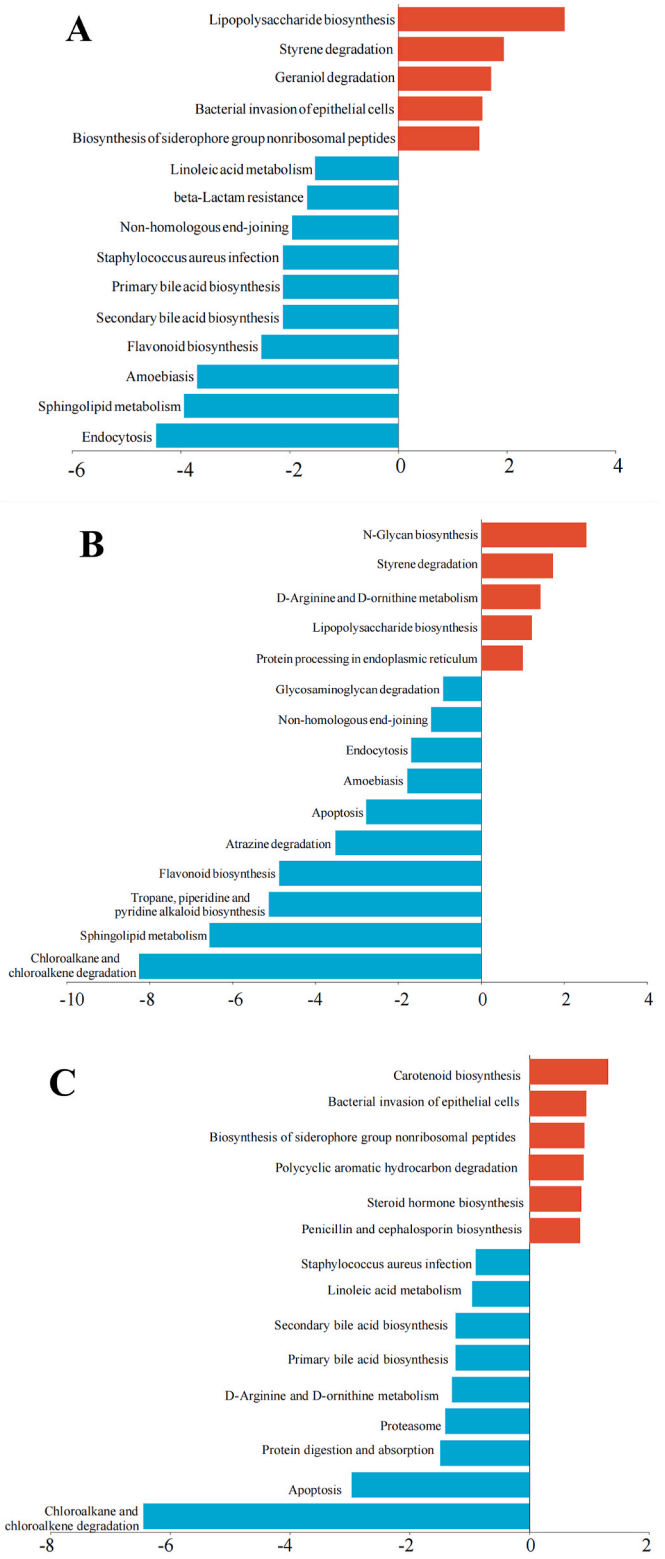

Fig. 5. Microbial functional prediction by PICRUSt analysis based on KEGG. (A) CAP group vs. ORS group; (B) CAP group vs. BLK group; (C) CAP group vs. INL group. The top 15 KEGG pathway terms were shown ($P < 0.05$).

increased OD_{600} value, as well as the decreased total carbohydrates/reducing sugar and the increased SCFAs indicated that CAP can be consumed by human gut microbiota. CAP modulated the composition and abundance of gut microbiota by promoting the growth of beneficial bacteria (*Megasphaera, Megamonas* and *Bifidobacterium*) and limiting the

development of harmful bacteria. What's more, acetic acid, *n*-butyric acid, *i*-valeric acid and *n*-valeric acid were the main SCFAs that were significantly enhanced by the fermentation of CAP. Microbial functional prediction results implied that CAP could significantly modulate the metabolism of the gut microbiota. All the findings revealed that the polysaccharides from the *C. axillaris* fruit have the potential to be utilized as prebiotics in functional foods. However, the fermentation properties and the regulation effect of gut microbiota of CAP *in vivo* need to be further studied.

CRediT authorship contribution statement

Jinjiao Dong: Methodology, Investigation, Data curation, Software, Writing – original draft, Writing – review & editing, Formal analysis. **Wenjun Wang:** Writing – review & editing. **Guodong Zheng:** Methodology, Formal analysis. **Nansheng Wu:** Writing – review & editing. **Jingjing Xie:** Software, Validation. **Shiyi Xiong:** Investigation, Methodology. **Panting Tian:** Resources. **Jingen Li:** Resources, Validation, Writing – review & editing, Funding acquisition, Supervision, Project administration.

Declaration of competing interest

The authors declare that they have no known competing financial interests or personal relationships that could have appeared to influence the work reported in this paper.

Data availability

The data that has been used is confidential.

Acknowledgments

This study was supported by Jiangxi Provincial Natural Science Foundation (20224BAB205044), and Provincial College Students' Innovation and Entrepreneurship Training Program (S202110410100). The authors also wish to thank Yanfang Liu from Shanghai Academy of Agricultural Sciences and Hui Zhang from University of Shanghai for Science and Technology for their technical supports in the HPAEC and HPSEC experiment.

References

Bai, Y., Zhou, Y., Zhang, R., Chen, Y., Wang, F., Zhang, M., 2023. Gut microbial fermentation promotes the intestinal anti-inflammatory activity of Chinese yam polysaccharides. Food Chem. 402, 134003 https://doi.org/10.1016/j.foodchem.2022.134003.

Chen, D., Chen, G.J., Wan, P., Hu, B., Chen, L.G., Ou, S.Y., et al., 2018. Digestion under saliva, simulated gastric and small intestinal conditions and fermentation in vitro by human intestinal microbiota of polysaccharides from Fuzhuan brick tea. Food Chem. 244, 331–339. https://doi.org/10.1016/j.foodchem.2017.10.074.

Chen, L., Wang, Y.X., Liu, J.X., Hong, Z.Y., Wong, K.H., Chiou, J.C., et al., 2023. Structural characteristics and in vitro fermentation patterns of polysaccharides from Boletus mushrooms. Food Funct. 14 (17), 7912–7923. https://doi.org/10.1039/d3fo01085f.

Feng, X.J., Bie, N.N., Li, J.Y., Zhang, M.L., Feng, Y.H., Ding, T.T., et al., 2022. Effect of in vitro simulated gastrointestinal digestion on the antioxidant activity, molecular weight, and microstructure of polysaccharides from Chinese yam. Int. J. Biol. Macromol. 207, 873–882. https://doi.org/10.1016/j.ijbiomac.2022.03.154.

Forbes, J.D., Chen, C.Y., Knox, N.C., Marrie, R.-A., El-Gabalawy, H., de Kievit, T., et al., 2018. A comparative study of the gut microbiota in immune-mediated inflammatory diseases-does a common dysbiosis exist? Microbiome 6 (1), 221. https://doi.org/10.1186/s40168-018-0603-4.

Fu, Y.P., Peng, X., Zhang, C.W., Jiang, Q.X., Li, C.Y., Paulsen, B.S., et al., 2023. Salvia miltiorrhiza polysaccharide and its related metabolite 5-methoxyindole-3-carboxaldehyde ameliorate experimental colitis by regulating Nrf2/Keap1 signaling pathway. Carbohydr. Polym. 306, 120626 https://doi.org/10.1016/j.carbpol.2023.120626.

Geng, X.R., Guo, D.D., Bau, T., Lei, J.Y., Xu, L.J., Cheng, Y.F., et al., 2023. Effects of in vitro digestion and fecal fermentation on physico-chemical properties and metabolic behavior of polysaccharides from Clitocybe squamulosa. Food Chem. X 18, 100644. https://doi.org/10.1016/j.fochx.2023.100644.

Gómez, B., Gullón, B., Yáñez, R., Schols, H., Alonso, J.L., 2016. Prebiotic potential of pectins and pectic oligosaccharides derived from lemon peel wastes and sugar beet pulp: a comparative evaluation. J. Funct.Foods 20, 108–121. https://doi.org/10.1016/j.jff.2015.10.029.

Guan, X.T., Feng, Y.J., Jiang, Y.Y., Hu, Y.Y., Zhang, J., Li, Z.P., et al., 2022. Simulated digestion and in vitro fermentation of a polysaccharide from lotus (Nelumbo nucifera Gaertn.) root residue by the human gut microbiota. Food Res. Int. 155, 111074 https://doi.org/10.1016/j.foodres.2022.111074.

Guo, D., Lei, J., He, C., Peng, Z., Liu, R., Pan, X., et al., 2022. In vitro digestion and fermentation by human fecal microbiota of polysaccharides from Clitocybe squamulose. Int. J. Biol. Macromol. 208, 343–355. https://doi.org/10.1016/j.ijbiomac.2022.03.126.

Han, X., Zhou, Q., Gao, Z., Lin, X., Zhou, K.X., Cheng, X.L., et al., 2022. In vitro digestion and fecal fermentation behaviors of polysaccharides from Ziziphus Jujuba cv. Pozao and its interaction with human gut microbiota. Food Res. Int. 162, 112022 https://doi.org/10.1016/j.foodres.2022.112022.

Hu, J.L., Nie, S.P., Min, F.F., Xie, M.Y., 2013. Artificial simulated saliva, gastric and intestinal digestion of polysaccharide from the seeds of Plantago asiatica L. Carbohydr. Polym. 92 (2), 1143–1150. https://doi.org/10.1016/j.carbpol.2012.10.072.

Huang, F., Hong, R.Y., Yi, Y., Bai, Y.J., Dong, L.H., Jia, X.C., et al., 2020. In vitro digestion and human gut microbiota fermentation of longan pulp polysaccharides as affected by Lactobacillus fermentum fermentation. Int. J. Biol. Macromol. 147, 363–368. https://doi.org/10.1016/j.ijbiomac.2020.01.059.

Kovatcheva-Datchary, P., Nilsson, A., Akrami, R., Lee, Ying S., De Vadder, F., Arora, T., et al., 2015. Dietary fiber-induced improvement in glucose metabolism is associated with increased abundance of prevotella. Cell Metabol. 22 (6), 971–982. https://doi.org/10.1016/j.cmet.2015.10.001.

Laparra, J.M., Sanz, Y., 2010. Interactions of gut microbiota with functional food components and nutraceuticals. Pharmacol. Res. 61 (3), 219–225. https://doi.org/10.1016/j.phrs.2009.11.001.

Li, D.T., Chen, R.C., Liu, J.Y., Liu, C.M., Deng, L.Z., Chen, J., 2022. Characterizing and alleviating the browning of Choerospondias axillaris fruit cake during drying. Food Control 132, 108522. https://doi.org/10.1016/j.foodcont.2021.108522.

Li, J.E., Dong, J.J., Xie, M.Z., Sui, W., Wu, N.S., 2024. The antioxidant, hypoglycemic and hypolipidemic effects of polysaccharides from choerospondias axillaris in vitro. Food Res. Dev. 45 (3), 59–66. https://doi.org/10.12161/j.issn.1005-6521.2024.03.009.

Li, J.E., Gong, Y., Luo, Y.Z., 2018. Study on extraction technology of polysaccharides from Choerospondias Axillaris fruit by Orthogonal test. J. Food Sci. Biotechnol. 37 (7), 754–757. https://doi.org/10.3969/j.issn.1673-1689.2018.07.013.

Li, J.E., Wang, W.J., Zheng, G.D., Li, L.Y., 2017a. Physicochemical properties and antioxidant activities of polysaccharides from Gynura procumbens leaves by fractional precipitation. Int. J. Biol. Macromol. 95, 719–724. https://doi.org/10.1016/j.ijbiomac.2016.11.113.

Li, J.E., Zhao, Y., Chen, Z., 2017b. Physicochemical properties and antioxidant activities of polysaccharides isolated from Choerospondias axillaris by ethanol fractional precipitation method. Sci. Technol. Food Ind. 38 (2), 132–135. https://doi.org/10.13386/j.issn1002-0306.2017.02.016.

Li, Q., Chen, J., Li, T., Liu, C., Liu, W., Liu, J., 2016. Comparison of Bioactivities and Phenolic Composition of Choerospondias Axillaris Peels and Fleshes, vol. 96, pp. 2462–2471. https://doi.org/10.1002/jsfa.7366, 7.

Li, X.J., Guo, R., Wu, X.J., Liu, X., Ai, L.Z., Sheng, Y., et al., 2020. Dynamic digestion of tamarind seed polysaccharide: indigestibility in gastrointestinal simulations and gut microbiota changes in vitro. Carbohydr. Polym. 239, 116194 https://doi.org/10.1016/j.carbpol.2020.116194.

Liang, Q., Vallance, B.A., 2021. What's for dinner? How Citrobacter rodentium's metabolism helps it thrive in the competitive gut. Curr. Opin. Microbiol. 63, 76–82. https://doi.org/10.1016/j.mib.2021.06.004.

Lv, K.L., Yuan, Q.X., Li, H., Li, T.T., Ma, H.Q., Gao, C.H., et al., 2022. Chlorella pyrenoidosa polysaccharides as a prebiotic to modulate gut microbiota: physicochemical properties and fermentation characteristics in vitro. Foods 11 (5), 725. https://doi.org/10.3390/foods11050725.

Ma, G.X., Xu, Q., Du, H.J., Muinde Kimatu, B., Su, A.X., Yang, W.J., et al., 2022. Characterization of polysaccharide from Pleurotus eryngii during simulated gastrointestinal digestion and fermentation. Food Chem. 370, 131303 https://doi.org/10.1016/j.foodchem.2021.131303.

Ma, Y., Jiang, S., Zeng, M., 2021. In vitro simulated digestion and fermentation characteristics of polysaccharide from oyster (Crassostrea gigas), and its effects on the gut microbiota. Food Res. Int. 149, 110646 https://doi.org/10.1016/j.foodres.2021.110646.

Mann, S., Chakraborty, D., Biswas, S., 2022. An alternative perspective of an underutilized fruit tree Choerospondias axillaris in health promotion and disease prevention: a review. Food Biosci. 47, 101609 https://doi.org/10.1016/j.fbio.2022.101609.

Miller, G.L., 1959. Use of dinitrosalicylic acid reagent for determination of reducing sugar. Anal. Chem. 31 (3), 426–428. https://doi.org/10.1021/ac60147a030.

Olm, M.R., Bhattacharya, N., Crits-Christoph, A., Firek, B.A., Baker, R., Song, Y.S., et al., 2019. Necrotizing enterocolitis is preceded by increased gut bacterial replication, Klebsiella, and fimbriae-encoding bacteria. Sci. Adv. 5 (12), eaax5727 https://doi.org/10.1126/sciadv.aax5727.

Oriach, C.S., Robertson, R.C., Stanton, C., Cryan, J.F., Dinan, T.G., 2016. Food for thought: the role of nutrition in the microbiota-gut–brain axis. Clin. Nutr. Exper. 6, 25–38. https://doi.org/10.1016/j.yclnex.2016.01.003.

Paliy, O., Kenche, H., Abernathy, F., Michail, S., 2009. High-throughput quantitative analysis of the human intestinal microbiota with a phylogenetic microarray. Appl. Environ. Microbiol. 75 (11), 3572–3579. https://doi.org/10.1128/aem.02764-08.

Pérez-Burillo, S., Molino, S., Navajas-Porras, B., Valverde-Moya, Á.J., Hinojosa-Nogueira, D., López-Maldonado, A., et al., 2021. An in vitro batch fermentation

protocol for studying the contribution of food to gut microbiota composition and functionality. Nat. Protoc. 16 (7), 3186–3209. https://doi.org/10.1038/s41596-021-00537-x.

Qiu, M., Dong, Y.H., Han, F., Qin, J.M., Zhang, H.N., Du, J.X., et al., 2016. Influence of total flavonoids derived fromChoerospondias axillaris foliumon aconitine-induced antiarrhythmic action and hemodynamics in Wistar rats. J. Toxicol. Environ. Health, Part A 79 (19), 878–883. https://doi.org/10.1080/15287394.2016.1193117.

Rao, T.P., Quartarone, G., 2019. Role of guar fiber in improving digestive health and function. Nutrition 59, 158–169. https://doi.org/10.1016/j.nut.2018.07.109.

Rui, Y., Wan, P., Chen, G., Xie, M., Sun, Y., Zeng, X., et al., 2019. Simulated digestion and fermentation in vitro by human gut microbiota of intra- and extra-cellular polysaccharides from Aspergillus cristatus. LWT 116, 108508. https://doi.org/10.1016/j.lwt.2019.108508.

Ruiz-Limon, P., Mena-Vazquez, N., Moreno-Indias, I., Manrique-Arija, S., Lisbona-Montanez, J.M., Cano-Garcia, L., et al., 2022. Collinsella is associated with cumulative inflammatory burden in an established rheumatoid arthritis cohort. Biomed. Pharmacother. 153, 113518 https://doi.org/10.1016/j.biopha.2022.113518.

Shang, Q.S., Jiang, H., Cai, C., Hao, J.J., Li, G.Y., Yu, G.L., 2018. Gut microbiota fermentation of marine polysaccharides and its effects on intestinal ecology: an overview. Carbohydr. Polym. 179, 173–185. https://doi.org/10.1016/j.carbpol.2017.09.059.

Sherwin, E., Dinan, T.G., Cryan, J.F., 2018. Recent developments in understanding the role of the gut microbiota in brain health and disease. Ann. N. Y. Acad. Sci. 1420 (1), 5–25. https://doi.org/10.1111/nyas.13416.

Sun, B., Xia, Q.M., Gao, Z.Y., 2014. Total flavones of Choerospondias axillaris attenuate cardiac dysfunction and myocardial interstitial fibrosis by modulating NF-κB signaling pathway. Cardiovasc. Toxicol. 15 (3), 283–289. https://doi.org/10.1007/s12012-014-9298-3.

Tian, J.J., Wang, X.M., Zhang, X.L., Chen, X.H., Dong, M.S., Rui, X., et al., 2023. Artificial simulated saliva, gastric and intestinal digestion and fermentation in vitro by human gut microbiota of intrapolysaccharide from Paecilomyces cicadae TJJ1213. Food Sci. Hum. Wellness 12 (2), 622–633. https://doi.org/10.1016/j.fshw.2022.07.065.

Wang, H., Gao, X.D., Zhou, G.C., Cai, L., Yao, W.B., 2008. In vitro and in vivo antioxidant activity of aqueous extract from Choerospondias axillaris fruit. Food Chem. 106 (3), 888–895. https://doi.org/10.1016/j.foodchem.2007.05.068.

Wu, D.-T., Yuan, Q., Guo, H., Fu, Y., Li, F., Wang, S.-P., et al., 2021. Dynamic changes of structural characteristics of snow chrysanthemum polysaccharides during in vitro digestion and fecal fermentation and related impacts on gut microbiota. Food Res. Int. 141, 109888 https://doi.org/10.1016/j.foodres.2020.109888.

Xie, A.Q., Wan, H., Feng, L., Yang, B.Y., Qun, W.Y., 2023. Protective effect of anoectochilus formosanus polysaccharide against cyclophosphamide-induced immunosuppression in BALB/c mice. Foods 12 (9), 1910. https://doi.org/10.3390/foods12091910.

Yin, C.M., Noratto, G.D., Fan, X.Z., Chen, Z.Y., Yao, F., Shi, D.F., et al., 2020. The impact of mushroom polysaccharides on gut microbiota and its beneficial effects to host: a review. Carbohydr. Polym. 250, 116942 https://doi.org/10.1016/j.carbpol.2020.116942.

Zhang, J., Li, X.Q., Zhao, K., Li, H.H., Liu, J.N., Da, S., et al., 2023. In vitro digestion and fermentation combined with microbiomics and metabolomics reveal the mechanism of superfine yak bone powder regulating lipid metabolism by altering human gut microbiota. Food Chem. 410, 135441 https://doi.org/10.1016/j.foodchem.2023.135441.

Zhang, W.Y., Hu, B., Liu, C., Hua, H.Y., Guo, Y.H., Cheng, Y.L., et al., 2022. Comprehensive analysis of Sparassis crispa polysaccharide characteristics during the in vitro digestion and fermentation model. Food Res. Int. 154, 111005 https://doi.org/10.1016/j.foodres.2022.111005.

Zhang, X., Aweya, J.J., Huang, Z.X., Kang, Z.Y., Bai, Z.H., Li, K.H., et al., 2020. In vitro fermentation of Gracilaria lemaneiformis sulfated polysaccharides and its agaro-oligosaccharides by human fecal inocula and its impact on microbiota. Carbohydr. Polym. 234, 115894 https://doi.org/10.1016/j.carbpol.2020.115894.

Zhou, W.T., Yan, Y.M., Mi, J., Zhang, H.C., Lu, L., Luo, Q., et al., 2018. Simulated digestion and fermentation in vitro by human gut microbiota of polysaccharides from bee collected pollen of Chinese Wolfberry. J. Agric. Food Chem. 66 (4), 898–907. https://doi.org/10.1021/acs.jafc.7b05546.